RESEARCH ARTICLE

**Editorial Process:** Submission:05/01/2024 Acceptance:02/07/2025

# *In vitro* Evaluation of Zinc Oxide-Metformin Folic Acid Nanocomposite as a Targeted Drug Delivery System for Cancer Therapy

**Nourhan Ezzat[1], Nagy Emadeldien[1], Miar Khaled Ali[1], Serene Fahd[1], Sarah Shebl[1], Malak Elshishiny[1], Mohamed Ramadan Gedamy[1], Nourhan Hassan[2], Soliman M. A. Soliman[3], Emad M. Elzayat[2]***

## Abstract

**Background:** Cancer has become the second cause of death worldwide after cardiovascular diseases. Thus, the development of efficient therapeutic approaches for cancer treatment seems necessary. One of the promising approaches is depending on nanotechnology in terms of drug delivery systems. ZnO nanoparticles have been approved for their efficiency as a drug delivery system due to their unique properties. Metformin (1, 1-dimethylbiguanide hydrochloride) is widely used as an anti-diabetic drug. However, recent studies have explored its repurposing as an anti-cancer drug. **Objective:** The present study aims to evaluate the feasibility and efficiency of a folic acid-metformin ZnO nanoparticle delivery system in the treatment of melanoma and bladder cancer cell lines. Methods: ZnO nanoparticles were chemically synthesized, loaded with metformin, and conjugated with folic acid at concentrations of 3% and 5%. Characterization of the nanoparticles was conducted using X-ray diffraction (XRD), Fourier-transform infrared spectroscopy (FTIR), dynamic light scattering (DLS), zeta potential analysis, and transmission electron microscopy (TEM). The cytotoxicity of ZnO nanoparticles was evaluated against human melanoma (A375) and bladder cancer (T24) cell lines via the MTT assay, with the determination of the half-maximal inhibitory concentration ($IC_{50}$). **Results:** ZnO nanoparticles were successfully synthesized with a spherical shape, size < 20 nm, and high homogeneity. Encapsulation efficiency of metformin on ZnO nanoparticles ranged from 95% to 98%. The folic acid-metformin ZnO nanoparticles demonstrated significant cytotoxic effects against both A375 and T24 cell lines in a dose-dependent manner. The $IC_{50}$ values revealed higher sensitivity of T24 bladder cancer cells compared to A375 melanoma cells. **Conclusion:** Overall, our study highlights the promise of the ZnO-metformin-folic acid nanoparticles as an efficient drug delivery system for cancer treatment. These results open up a potentially valuable line of novel therapeutic applications.

**Keywords:** ZnO nanoparticles- Metformin- Folic acid- Drug delivery system- Repurposing drug- Anti-cancer activity

*Asian Pac J Cancer Prev,* **26 (2)**, 443-452

## Introduction

Cancer is considered a major cause of mortality and morbidity all over the world as it is the world's 2nd leading cause of death [1]. It is a critical public health problem and a significant obstacle to extending life expectancy as by 2020 cancer-related deaths reached 10 million according to a WHO report and are expected to be raised to 16.4 million per year by 2040. Despite considerable advancements in treatment modalities such as chemotherapy, radiotherapy, hormonal therapy, immunotherapy, and surgeries, conventional therapies [2, 3]. are not only specific to cancer cells but also, affect normal cells [3]. So, targeted drug therapy that delivers the drug to tumors while leaving normal cells unaffected has gained a great concern in cancer treatment [4]. In this context, nanotechnology is gaining attraction as a medical discipline with the potential to provide considerable therapeutic benefits [2]. There have been several notable applications of nanomedicine (chemotherapeutic agents, biological agents, immunotherapeutic agents, etc.) in the treatment of various diseases in recent years [5]. Among these nanostructures, metal oxide nanoparticles have shown promise as drug delivery, targeted gene delivery, and tumor imaging vehicles [6, 7].

ZnO nanoparticles are being used successfully in drug delivery, targeted gene delivery, and tumor imaging [8]. ZnO NPs possess several attributes that render them

*[1]Biotechnology/ Biomolecular Chemistry Program, Faculty of Science, Cairo University, Giza, Egypt. [2]Biotechnology Department, Faculty of Science, Cairo University, Giza, Egypt. [3]Chemistry Department, Faculty of Science, Cairo University, Giza, Egypt. *For Correspondence: elzayatem@sci.cu.edu.eg*

highly suitable for anticancer therapy [9]. ZnO NPs have a reasonably high biocompatibility, confirmed by the FDA recognition as generally recognized as safe (GRAS), which makes them favorable for biomedical uses. The administered ZnO is easily biodegradable or can participate in the body's active nutritional cycle [10, 9]. Moreover, when compared to other nanoparticles, ZnO NPs have an inherent property of selective cytotoxicity against cancerous cells in vitro, which is crucial for targeted therapy [9, 11]. The synthesis of ZnO NPs is relatively simple with a number of different methods available [9]. ZnO NPs can be produced using either conventional (Physical, Chemical, and Biological (green) synthesis techniques) or non-conventional methods (microfluidic reactor-based synthesis), which helps in controlling their size and distribution in order to enhance their therapeutic efficacy [12, 13]. Furthermore, the semiconductor property of ZnO NPs enables the induction of oxidative stress in cancer cells through ROS generation, contributing to their cytotoxicity effects [14, 9].

Drug repurposing, which is also known as drug repositioning, reprofiling, or re-tasking, is an additional approach to cancer therapy that figures out novel applications for currently approved or investigational drugs outside of their intended therapeutic indications [15, 16]. This approach has several advantages including fewer development risks and shorter timeframes, as safety profiles and formulation groundwork are often established [17, 18]. Metformin (MET) (1, 1-dimethylbiguanide hydrochloride), a widely used medication for type II diabetes patients, has emerged as a promising candidate for cancer therapy [19]. Beyond its antidiabetic effects, metformin demonstrates potent antineoplastic properties, mediated through mechanisms including cell cycle regulation, epigenetic alterations, and immunomodulation [20, 21]. Metformin (MET) (1, 1-dimethylbiguanide hydrochloride), a widely used medication for type II diabetes patients, has emerged as a promising candidate for cancer therapy [19]. Patients with type II diabetes who took the medication revealed a significant reduction in cancer-related mortality and significant inhibition of the growth malignancies [20, 21].

In addition to the role of metformin as an anti-diabetic drug, it also has anti-neoplastic activities, mediated through various mechanisms including cell growth suppression, cell cycle regulation, epigenetic alterations, and activation of immunomodulation. There are numerous ways that metformin works including reducing the activity of the mitochondrial respiratory chain, triggering AMP-activated protein kinase (AMPK) and the phosphatidylinositol 3-kinase (PI3K) signaling, adjusting insulin pathways, and promoting autophagy [22-24]. Metformin also enhances reactive oxygen species (ROS) accumulation and stimulates redox signaling mechanisms [22, 25]. Additionally, metformin influences epigenetic processes, impacting DNA methylation, histone acetylation, and microRNA expression, all of which play pivotal roles in cancer development and progression [22, 25-28]. Metformin has been reported to affect DNA methylation via the methionine cycle intermediate S-adenosylmethionine (SAM). Moreover, metformin-induced metabolic changes from TCA cycle intermediates such as acetyl-CoA contribute to histone and non-histone acetylation [22, 28]. Metformin inhibited tumor growth via modulating the Dicer processing enzyme, which was followed by alterations in a subset of miRNAs.

Furthermore, the utilization of targeting molecules such as folate in drug delivery systems holds promise for enhancing specificity and efficacy in cancer treatment [29, 30]. Folate-modified nanoparticles have demonstrated the ability to selectively target cancer cells, representing a significant advancement in tumor-targeted therapy [31-35]. In summary, the combination of nanotechnology, medication repurposing, and targeted drug delivery techniques offers a multimodal approach to cancer treatment, reducing side effects and providing new opportunities for enhanced therapeutic outcomes. This study explores the potential of metformin-loaded zinc oxide nanoparticles combined with folate-targeted drug delivery strategies to advance cancer treatment paradigms, offering innovative insights into enhancing therapeutic efficacy and specificity.

## Materials and Methods

*Chemicals and Reagents*

The chemicals used in this study included ZnSO4 (cat. no. 7733-02-0), NaOH (cat. no. 1310-73-2, and Folic acid (cat. no. 59-30-3) (Sigma-Aldrich, Germany), Metformin (Merck Santé, cat. no. 1115-70-4, France). T24 (bladder carcinoma) and A375 (melanoma) cell lines, and human normal fibroblasts (HBF4) were obtained from Nawah Scientific, Egypt. Culture media and reagents including DMEM (cat. no. LM-D1111), PBS (cat. no. LM-S2043), Trypsin-EDTA 1X (cat. no. LM-T1705) were sourced from Biosera, Germany, while SDS (cat. no. 151-21-3) and MTT (cat. no. 298-93-1) were provided from Sigma-Aldrich, Germany. The successful synthesis of ZnO NPs was confirmed through various analytical techniques. FTIR was conducted to characterize ZnO NPs using a Testcan Shimadzu Infra-Red spectrophotometer (model 8000) employing the KBr pressed disk method, with a scanning range of 4000–600 $cm^{-1}$. XRD was used to determine ZnO patterns using a PANalytical X'Pert Pro instrument, operating at tube voltages and currents of 45 kV and 40 mA, respectively. Additionally, dynamic light scattering (DLS) and zeta potential analyses were carried out to further characterize the synthesized nanoparticles.

*Synthesis and Characterization of ZnO NPs*

ZnO NPs were synthesized from aqueous solutions of ZnSO4 and NaOH. Initially, each solution was dissolved separately on the magnetic stirrer until clarity. Subsequently, NaOH was added drop by drop to ZnSO4 solution, the mixture was left on the magnetic stirrer overnight. Following the reaction, the solution was washed until reaching a neutral pH to remove any residual impurities. The resulting solution was then subjected to heat in an oven at 100˚C for 2 hours to obtain dried nanoparticles, which were then processed through grinding to achieve uniform particle size distribution. Characterization of the synthesized ZnO NPs was

performed to confirm their formation. XRD was conducted to determine the crystalline structure of the nanoparticles. FTIR was employed to investigate the chemical bonds present in nanoparticles. Particle size analysis and zeta potential were carried out to assess the size distribution and surface charge of the nanoparticles, respectively., Additionally, Transmission electron microscopy (TEM) was utilized to visualize the morphology and size of the nanoparticles at the nanoscale level. [36, 37].

*Drug Loading*

To load the metformin drug into ZnO NPs (total = 0.4 gm), two separate solutions were prepared by dissolving 0.006 and 0.01 g of metformin in 60 ml of distilled water, resulting in concentrations of 3% and 5% relative to ZnO NPs, respectively), Each solution was mixed with 0.2 g of ZnO NPs and stirred on a magnetic stirrer for 30 minutes at room temperature; then, the solution was incubated overnight. The resulting solution was centrifuged at 8000 rpm for 10 minutes for separation. After centrifugation, the supernatant containing unbound metformin was discarded, and the pellet containing the metformin-loaded ZnO NPs was dried in an oven at 40˚C for 2 hours. Confirmation of successful drug loading onto the NPs was achieved through FTIR. Encapsulation efficiency was calculated after measuring the absorbance of the metformin solution before and after loading onto the ZnO NPs, ZnO metformin folic acid nanocomposite was prepared by adding 0.1 gm of folic acid to a solution containing ZnO-MET (0.02 gm dissolved in 100 ml distilled water) for two different concentrations. The mixture was stirred on a magnetic stirrer for 6 hours at 60˚C. Following stirring, it was centrifuged for 10 minutes at 6000 rpm, and the pellet was washed with distilled water before dried in the oven.

*Cell Culture*

Cell lines were cultivated and subjected to MTT assay to evaluate cell viability after the treatment to assess the anticancer activity of ZnO NPs, and metformin loaded on ZnO NPs compared to free metformin. The T24 and A375 cell lines were cultured using DMEM media. Before splitting, the old medium was removed, and cells were washed with PBS. Subsequently, trypsin was added for cell detachment, followed by a short incubation period of 5 minutes at 37°C. After incubation, a small volume of media that contains FBS was added to inhibit trypsin and antibiotic activities. The detached cells were then transferred into larger flasks and the volume was adjusted to 10 ml with fresh medium. The cells were then incubated until reaching approximately 80% confluence. Cell counting was performed using a hemocytometer. After trypsinization, cells were collected into a falcon tube and centrifuged to obtain a cell pellet. The pellet was suspended in 1 ml of medium and diluted with PBS at a 1:10 ratio. Subsequently, 10 µl of the diluted suspension was mixed with 10 µl of trypan blue stain, and the mixture was loaded into each chamber of the hemocytometer for counting. Following cell counting, ELISA plates containing 96 wells were utilized for cell seeding, with 10,000 cells in each well. Two plates were prepared for each cell line. The plates were then incubated overnight at 37°C with 5% CO2. Routine mycoplasma testing was performed using PCR to confirm the absence of contamination, ensuring the integrity and reliability of cell cultures.

*In Vitro Cytotoxicity assay*

Cell treatment involved the application of ZnO NPs, free MET, ZnO-MET (3% and 5%), and ZnO-MET folic acid (3% and 5%) across two cell lines. Various concentrations (100, 50, 25, 12.5, 6.25 µg/ml) of each treatment were applied to cells in four replicates and incubated for 48 hours to assess their cytotoxic effects using the MTT (3-[4,5-dimethylthiazol-2yl]-2,5-diphenyl tetrazolium bromide) assay. Following the incubation period, the media were aspirated, and 100 µl of MTT solution was added to each well, followed by further incubation at 37°C for 4 hours. Subsequently, 20% sodium dodecyl sulfate (SDS) was added to dissolve the insoluble purple formazan product, forming a colored solution, which was then incubated for an additional 30 minutes. Finally, the absorbance of the colored solution was measured at 492 nm using an ELISA reader. The relative viability of the cells was calculated by comparing the optical density (OD) of the treated cells to that of the control cells, using the formula: (OD test / OD control) × 100. The half-maximal inhibitory concentration ($IC_{50}$) was determined using graph pad prism software.

*Releasing kinetics*

The drug release kinetics were assessed using the dialysis bag method, a well-established technique wherein drug-loaded carriers are physically separated from the bulk media by a semipermeable dialysis membrane, allowing the release to be monitored over time. A suspension containing 20 mg of the drug in 10 ml of phosphate-buffered saline (PBS) at pH 7.4 was prepared. Subsequently, 1 ml of the suspension was carefully transferred into a dialysis bag with a molecular weight cutoff of 12-14 kDa. The dialysis bag was securely sealed at both ends to prevent any leakage of the drug suspension. The dialysis bag was then immersed in 20 ml of PBS solution and incubated for 72 hours. The whole system was placed in a shaking incubator at 100 rpm at 37°C. Lastly, 1 ml samples of the medium surrounding the dialysis bag were collected and immediately replaced with an equal volume of fresh PBS to maintain sink conditions. The collected samples were then analyzed using a UV spectrophotometer at a wavelength of 234 nm.

## Results

*Release test*

The outcomes of the release test were conducted for the ZnO-MET folic acid nanoparticles at a concentration of 5%. The experiment was performed in triplicate, and the average of these replicates was calculated for clarity and accuracy of representation. Analysis of the release profile reveals that the highest amount of drug release, approximately 0.6 mg, was observed at the 24 hours following the start of the release test (Figure 1A).

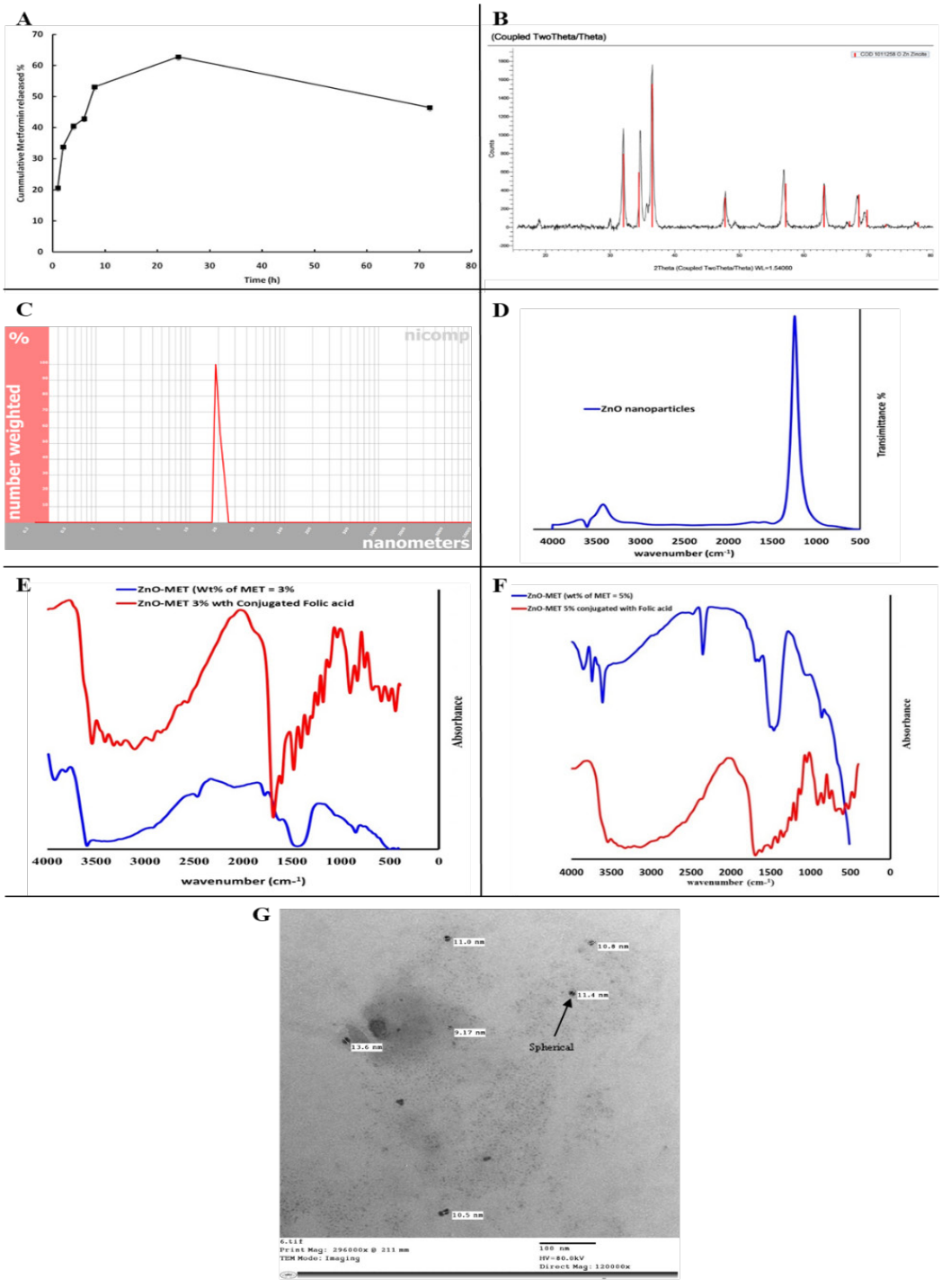


Figure 1. Characterization of Nanoparticles. (A) Illustration of cumulative metformin release %, (B) XRD pattern of prepared ZnO nanoparticles, (C) Particle size of ZnO nanoparticle, (D) FTIR of ZnO NPs, (E) FTIR of ZnO loaded with metformin 3% (blue line) and ZnO loaded with metformin 3% conjugated with folic acid (red line) and (F) FTIR of ZnO loaded with metformin 5% (blue line) and FTIR of ZnO loaded with metformin 5% conjugated with folic acid (red line), and (G) TEM image shows ZnO NPs loaded with metformin 5% conjugated with folic acid size (~11.08 nm), shape (spherical), and homogeneity in terms of size and shape.

Subsequently, a gradual decline in drug release was observed, persisting until the conclusion of the 72-hour test duration. These results highlight the dynamics of the drug release from the ZnO-MET folic acid nanoparticles, showing sustained release kinetics during the test after an initial release. This would be essential to understanding the regulated release behavior of NPs and maximizing their therapeutic efficacy.

*Characterization of nanoparticles*

By carefully analyzing the XRD patterns, we were able to identify important variables including peak intensity, position, and width in addition to figuring out the full width at half maximum (FWHM) data (Figure 1B). The distinct peaks observed in the XRD pattern, located at 32.071°, 34.467°, 36.534°, 47.790°, 57.168°, 63.103°, 67.072°, and 68.493°, have been identified as hexagonal

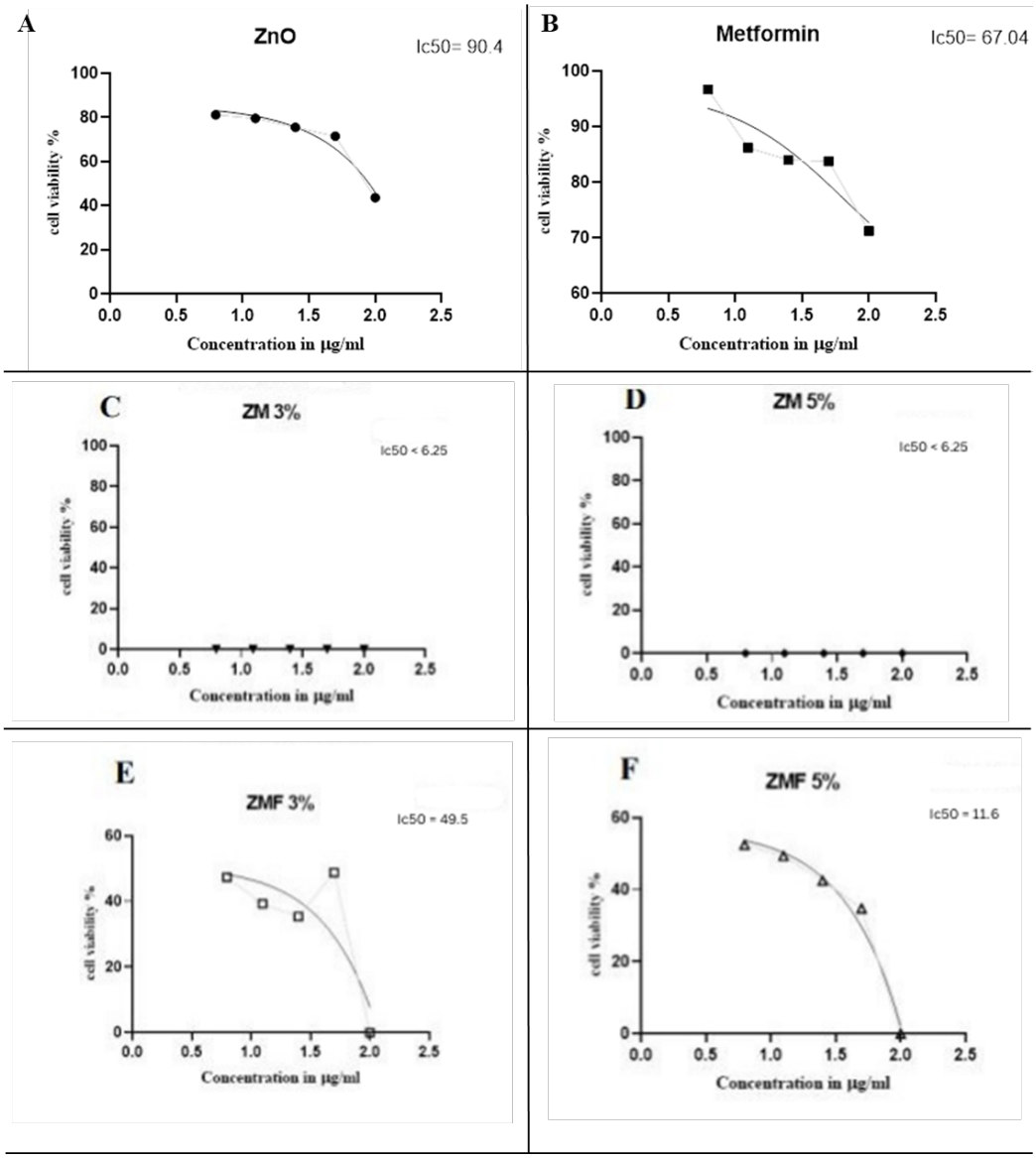


Figure 2. Anticancer Effect of Free MET, ZnO, ZnO-MET (3% and 5%), and ZnO-MET Folic Acid (3% and 5%) against the Human A375 Melanoma Cell Line. (A) $IC_{50}$ of ZnO, (B) MET, (C) ZnO-MET (ZM) 3%, (D) ZnO-MET (ZM) 5%, (E) ZnO-MET folic acid (ZMF) 3%, and (F) ZnO-MET folic acid (ZMF) 5%.

wurtzite phase of ZnO with lattice constants. It also shows the produced NP was devoid of impurities since it lacks any XRD peaks other than ZnO peaks [44]. This observation confirms the successful synthesis of high-quality pure ZnO nanoparticles thereby confirming their suitability for various applications in nanotechnology and biomedicine [38].

Before assessing the zeta potential of ZnO NPs in aqueous systems, it is important to evaluate the particle size distribution of ZnO NPs dispersed in deionized (DI) water. As shown in Figure 1C, the ZnO NPs exhibited a particle size of approximately 20 nm. Furthermore, microscopic examination revealed the morphologies of the ZnO NPs to be round-like [39]. These observations provide essential insights into the physical characteristics of the ZnO NPs, laying the groundwork for subsequent analyses.

Following three independent measurements of ZnO NPs, the average zeta potential value was determined to be +3.04 mV [39]. This characterization provides valuable insights into the electrostatic properties of the ZnO NPs, indicating a slight positive surface charge under the experimental conditions. Such information is crucial in understanding the stability, dispersion, and interactions of the nanoparticles in aqueous environments.

In our investigation, FTIR measurements were conducted to corroborate the formation of various nanoparticle formulations, including pure ZnO, ZnO loaded with 3% and 5% metformin (ZnO-MET), and ZnO loaded with 3% and 5% metformin, and conjugated with 0.1 gm of folic acid (ZnO-MET folic acid), as illustrated in Figure 1D [40]. Characteristic absorption bands corresponding to ZnO were discerned within the spectral range of 1000 to 4000 $cm^{-1}$, indicative of carboxylate and hydroxyl impurities present in the materials. A broad band observed at 3608.77 $cm^{-1}$ was attributed to the O-H stretching mode of hydroxyl groups, while the peak at 2777.76 $cm^{-1}$ arose from C-H

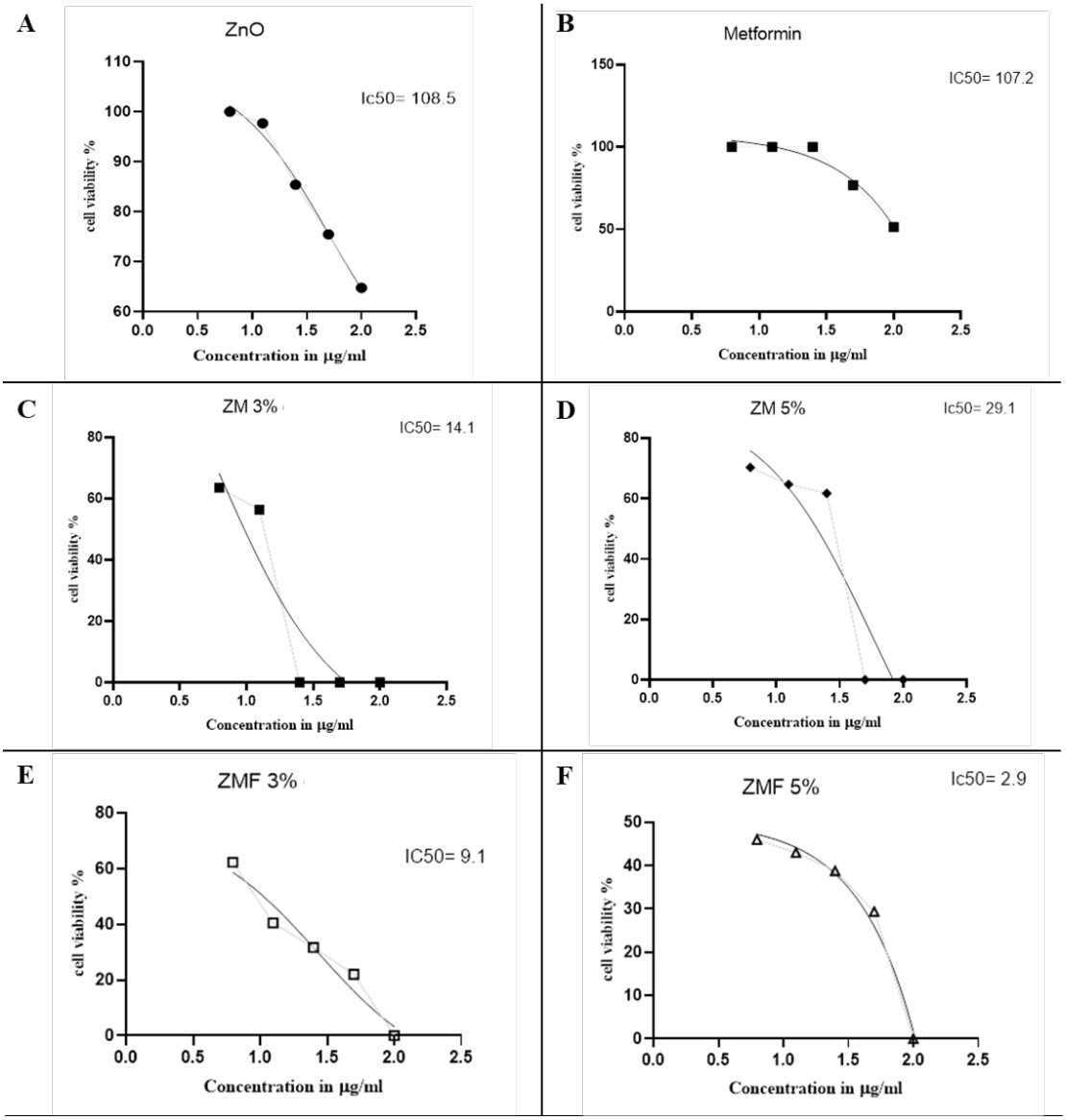


Figure 3. Anticancer Efficacy of Free MET, ZnO, ZnO-MET (3% and 5%), and ZnO-MET Folic Acid (3% and 5%) against the Human T24 Bladder Cell Line. (A) $IC_{50}$ of ZnO, (B) MET, (C) ZnO-MET (ZM) 3%, (D) ZnO-MET (ZM) 5%, (E) ZnO-MET folic acid (ZMF) 3%, and (F) ZnO-MET folic acid (ZMF) 5%.

stretching vibrations of alkane groups. Peaks at 1655.20 $cm^{-1}$ and 1495.85 $cm^{-1}$ were associated with the oxide in ZnO and the asymmetrical and symmetrical stretching of zinc carboxylate, respectively. Interestingly, a trend was observed where the content of carboxylate (COO-) and hydroxyl (-OH) groups decreased with increasing nanoparticle size. This suggests a diminishing presence of these FTIR-identified impurities near the surfaces of ZnO nanoparticles [41].

After the loading of particles with metformin, recharacterization was performed using FTIR (Figure 1E). Significantly, the intensity of the ZnO band exhibited a decrease following doping with metformin (ZnO-MET), attributed to the incorporation of metformin into the ZnO crystal structure [40]. In the FTIR spectrum of metformin HCl, principal absorption peaks emerged between 3500 to 3000 $cm^{-1}$, attributed to the amine (N-H) groups present in metformin. Additionally, peaks around 2900 and 1470 $cm^{-1}$ were observed, corresponding to the methyl (CH3) groups [42]. Subsequent conjugation with folic acid led to recharacterization (Figure 1F). It was noted that when folic acid conjugates with ZnO and metformin, small shifts in peak positions were observed with respect to pure ZnO nanoparticles. Specifically, shifts occurred between 3320 and 3200 $cm^{-1}$ for amine (N-H) groups, while a peak around 3100 $cm^{-1}$ was attributed to C-H aromatic stretching. Additionally, a peak at 762 $cm^{-1}$ was observed, indicative of C-H bending / N-H rocking. Moreover, a new mid-strong absorption band significantly emerged around 2300 $cm^{-1}$, attributed to the N+–H stretching vibration band of C=N+H– on the PT ring [43]. These FTIR recharacterizations provide information into the structural modifications undergone by the nanoparticles following metformin loading and subsequent conjugation with folic acid, offering further elucidation of their chemical compositions and functional groups.

Figure 1G represents the TEM analysis images of the ZnO nanoparticles loaded with 5% metformin

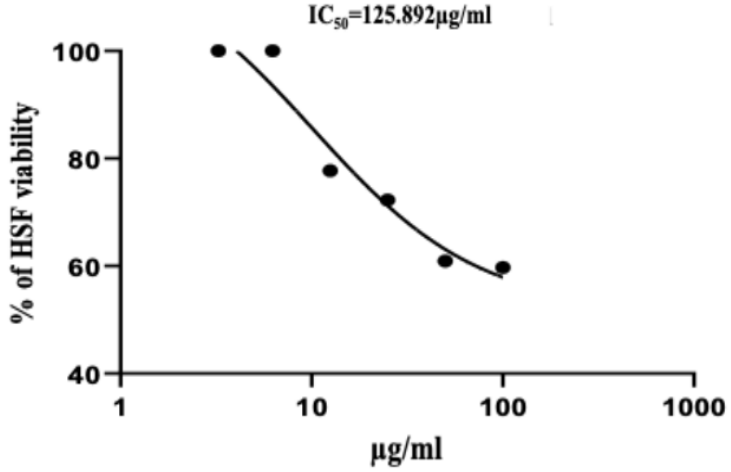


Figure 4. Anticancer Efficacy of ZnO-MET Folic Acid (5%) against the Human Normal Fibroblasts (HBF4).

Table 1. Encapsulation Efficiency. This table shows that metformin 3% was encapsulated in ZnO NPs by 95% and metformin 5% was encapsulated in ZnO NPs by 98%

| Encapsulation efficiency | Abs. of metformin after addition of NPs | Abs. of metformin before addition of NPs | Maximum Wavelength (nm) of MET | Wt% of MET loaded onto ZnO nanoparticles |
|---|---|---|---|---|
| 95% | 0.087 | 2.17 | 220 | 3% |
| 98% | 0.023 | 2.18 | 220 | 5% |

and conjugated with folic acid nanocomposite. These images offer a detailed glimpse into the morphological characteristics and structural features of the synthesized nanocomposite, providing valuable insights into its size, shape, and distribution.

*Encapsulation Efficiency*

To quantify the extent of metformin encapsulation within the ZnO NPs, encapsulation efficiency was measured. The percentage of drug loading was calculated using the following equation: [(X-Y)/X] *100. Here, X represents the absorbance before encapsulation, and Y represents the absorbance after encapsulation [44]. In our study, encapsulation efficiency measurements revealed high values, with 95% and 98% efficiency observed for ZnO NPs loaded with 3% and 5% metformin, respectively. The absorbance values after the addition of NPs were 0.087 and 0.023, while the absorbance values before the addition of NPs were 2.17 and 2.18 for 3% and 5% metformin loading, respectively (Table 1). Furthermore, the maximum wavelength (nm) of metformin was determined to be 220. These results indicate successful encapsulation of metformin into the ZnO nanoparticles, with weight percentages of 3% and 5% loaded onto the nanoparticles.

*Cytotoxic assay*

The cytotoxic efficiency of all nanocomposites compared to free MET against human cancerous A375 and T24 cells was investigated using the MTT assay. As shown in Figure 2, the anticancer effect of free MET, ZnO, ZnO-MET (3% and 5%), and ZnO-MET folic acid (3% and 5%) against the human A375 melanoma cell line was evaluated. The $IC_{50}$ values were determined for each nanocomposite, with free MET exhibiting an $IC_{50}$ of 67.04 µg/ml, ZnO at 90 µg/ml, ZnO-MET (3%) at 25 µg/ml, ZnO-MET (5%) at 25 µg/ml, ZnO-MET folic acid (3%) at 49.5 µg/ml, and ZnO-MET folic acid (5%) at 11.6 µg/ml, respectively. On the other hand, Figure 3 illustrates the anticancer efficacy of free MET, ZnO, ZnO-MET (3% and 5%), and ZnO-MET folic acid (3% and 5%) against the human T24 bladder cell line. The $IC_{50}$ values were determined for each nanocomposite, with free MET displaying an $IC_{50}$ of 107.2 µg/ml, ZnO at 108.5 µg/ml, ZnO-MET (3%) at 14.1 µg/ml, ZnO-MET (5%) at 29.1 µg/ml, ZnO-MET folic acid (3%) at 9.1 µg/ml, and ZnO-MET folic acid (5%) at 2.9 µg/ml, respectively. Moreover, depending on the $IC_{50}$ of ZnO-MET folic acid (5%) with HBF4 normal cells (Figure 4), the selectivity index (SI) for A375 and T24 cell lines are 10.85 and 43.41, respectively. These findings highlight the superior efficacy of ZnO-MET folic acid (5%) among the tested nanocomposites in A375 and T24 cell lines, as demonstrated by its significantly lower $IC_{50}$ value of 11.6 and 2.9 µg/ml, respectively. These results position ZnO-MET folic acid (5%) as a promising therapeutic candidate for further development and exploration as a potent anticancer therapeutic agent.

## Discussion

Repurposing drugs has recently gained significant attention, with metformin emerging as an outstanding candidate [45, 46]. In addition to its major effect in treating type II diabetes, it has been known to act as an anti-cancer drug through various mechanisms of action [47, 48]. The present study aimed to evaluate the

effectiveness of a novel drug delivery system utilizing ZnO nanoparticles loaded with metformin and conjugated with folic acid for in vitro application against different cancer cell lines, human melanoma (A375) and bladder cancer (T24) cell lines. Physicochemical analyses, including XRD, DLS, and FTIR, revealed the unique characteristics of ZnO nanoparticles in terms of shape and size [39, 38, 41]. Moreover, FTIR analysis and TEM supported the encapsulation efficiency of metformin on ZnO nanoparticles [42], with loading efficiencies ranging from 95% to 98%. Additionally, FTIR graphs provided evidence of successful conjugation with folic acid [43]. These characterization methods confirm the successful fabrication of ZnO NPs loaded with metformin and conjugated with folic acid.

Our study also demonstrated the enhanced cytotoxicity of ZnO NPs loaded with metformin and folic acid compared to ZnO NPs and free metformin alone. Notably, ZnO nanoparticles and free metformin are cytotoxic to different degrees, with the most significant effect observed on the A375 cell line. Loading ZnO nanoparticles with metformin significantly enhanced cytotoxicity, with the 3% concentration demonstrating the best effect on the T24 cell line ($IC_{50}$ = 14.1 μg/ml) and the 5% concentration exhibiting the strongest effect on the A375 cell line ($IC_{50}$ = 25 μg/ml).

Conjugation of folic acid to ZnO metformin nanocomposite further increased the sensitivity to both cancer cell lines, with the best effect on the T24 cell line, where the $IC_{50}$ was reduced from 29.1 μg/ml to 2.9 μg/ml. This indicates an increase in the sensitivity by tenfold highlighting the efficacy of folic acid in targeting cancer cells. However, in human melanoma (A375) cell line $IC_{50}$ was reduced from 25 μg/ml to 11.6 μg/ml.

Our findings suggest that the cytotoxic effects of ZnO NPs, the anticancer activity of metformin, and the targeting effect of folic acid contribute to the efficacy of our drug delivery system. Previous studies have highlighted the selective cytotoxicity of ZnO nanoparticles to cancer cells and the anticancer properties of metformin, showing that ZnO NPs exhibit 28–35 times greater selective cytotoxicity for cancer cells than normal cell toxicity [49]. This selective property comes from the higher production of ROS in tumor cells than in normal cells after applying the ZnO NPs. The redox nature of ZnO NPs reacts with various signaling molecules and ROS present in cancer cells causing increased oxidative stress leading to cell death [8]. Moreover, the overexpression of folate receptors in many cancer cells underscores the importance of folic acid conjugation in targeting cancer cells. In addition, metformin has also shown unique anti-cancer activity besides its well-known anti-diabetic effect. It induces cell death by many mechanisms of action, such as cell growth suppression, epigenetic modification, and immunoregulation [20, 21]. Many cancer cells are reported to highly express folate receptors [32]. In this context, the present study showed that folic acid conjugation increased the cytotoxic effect of ZnO/metformin in both melanoma and bladder cancer cell lines, with the latter being the most sensitive. The present data run in contradiction with a previous study [50], which reported that epithelial cancer cells highly express folate receptors than bladder cancer cells. This may be due to the fact that folic acid is in physical not chemical interaction with ZnO NPs, which suggests that it may not conjugate with ZnO NPs in the fixed orientation needed to bind to the folate receptor accurately. This may also affect the rate of release of metformin from the composite.

Given the present data, one can claim that ZnO NPs conjugated with metformin folic acid drug delivery system may be a successful targeted therapy for cancer. However, further investigations seem necessary to confirm the present results.

In conclusion, our study highlights the potential of ZnO nanoparticles loaded with metformin and conjugated with folic acid as a promising targeted therapy for various types of cancer. Our investigation focused on assessing the therapeutic effect of ZnO nanoparticles loaded with metformin and conjugated with folic acid against two cancer cell lines: T24 (human bladder cancer) and A375 (human melanoma). Our findings indicate that conjugation at a 5% concentration significantly enhanced the targeting efficiency of cancer cells in both cell lines. Notably, the $IC_{50}$ value for the T24 cell line was reduced from 29.1 μg/ml to 2.9 μg/ml, underscoring the potent efficacy of the conjugate. However, further in vitro and in vivo studies, along with comprehensive analyses, are suggested to validate and prove the full therapeutic potential of this drug delivery system. Future research efforts should explore the mechanism of action, pharmacokinetics, and toxicity profiles to open the way for potential clinical applications in cancer treatment.

## Author Contribution Statement

All authors contributed equally in this study.

## Acknowledgements

None.

*Conflicts of interest*

The authors declare no conflict of interest.

## References

1. Mattiuzzi C, Lippi G. Current cancer epidemiology. J Epidemiol Glob Health. 2019;9(4):217-22. https://doi.org/10.2991/jegh.k.191008.001.
2. Anjum S, Ishaque S, Fatima H, Farooq W, Hano C, Abbasi BH, et al. Emerging applications of nanotechnology in healthcare systems: Grand challenges and perspectives. Pharmaceuticals (Basel). 2021;14(8). https://doi.org/10.3390/ph14080707.
3. Cheng Z, Li M, Dey R, Chen Y. Nanomaterials for cancer therapy: Current progress and perspectives. J Hematol Oncol. 2021;14(1):85. https://doi.org/10.1186/s13045-021-01096-0.
4. Yao Y, Zhou Y, Liu L, Xu Y, Chen Q, Wang Y, et al. Nanoparticle-based drug delivery in cancer therapy and its role in overcoming drug resistance. Front Mol Biosci. 2020;7:193. https://doi.org/10.3389/fmolb.2020.00193.
5. Patra JK, Das G, Fraceto LF, Campos EVR, Rodriguez-Torres MDP, Acosta-Torres LS, et al. Nano based drug delivery

systems: Recent developments and future prospects. J Nanobiotechnology. 2018;16(1):71. https://doi.org/10.1186/s12951-018-0392-8.
6. Singh KR, Nayak V, Singh J, Singh AK, Singh RP. Potentialities of bioinspired metal and metal oxide nanoparticles in biomedical sciences. RSC Adv. 2021;11(40):24722-46. https://doi.org/10.1039/d1ra04273d.
7. Rasmussen JW, Martinez E, Louka P, Wingett DG. Zinc oxide nanoparticles for selective destruction of tumor cells and potential for drug delivery applications. Expert Opin Drug Deliv. 2010;7(9):1063-77. https://doi.org/10.1517/17425247.2010.502560.
8. Anjum S, Hashim M, Malik SA, Khan M, Lorenzo JM, Abbasi BH, et al. Recent advances in zinc oxide nanoparticles (zno nps) for cancer diagnosis, target drug delivery, and treatment. Cancers (Basel). 2021;13(18). https://doi.org/10.3390/cancers13184570.
9. Bisht G, Rayamajhi S. Zno nanoparticles: A promising anticancer agent. Nanobiomedicine (Rij). 2016;3:9. https://doi.org/10.5772/63437.
10. Ali A, Phull AR, Zia M. Elemental zinc to zinc nanoparticles: Is ZnO NPs crucial for life? Synthesis, toxicological, and environmental concerns. Nanotechnology Reviews. 2018 Oct 25;7(5):413-41. https://doi.org/10.1515/ntrev-2018-0067.
11. Tanino R, Amano Y, Tong X, Sun R, Tsubata Y, Harada M, et al. Anticancer activity of zno nanoparticles against human small-cell lung cancer in an orthotopic mouse model. Mol Cancer Ther. 2020;19(2):502-12. https://doi.org/10.1158/1535-7163.MCT-19-0018.
12. Agarwal H, Kumar SV, Rajeshkumar S. A review on green synthesis of zinc oxide nanoparticles–An eco-friendly approach. Resource-Efficient Technologies. 2017 Dec 1;3(4):406-13. https://doi.org/10.1016/j.reffit.2017.03.002
13. Jin SE, Jin HE. Synthesis, characterization, and three-dimensional structure generation of zinc oxide-based nanomedicine for biomedical applications. Pharmaceutics. 2019;11(11). https://doi.org/10.3390/pharmaceutics11110575.
14. Sanati M, Afshari AR, Kesharwani P, Sukhorukov VN, Sahebkar A. Recent trends in the application of nanoparticles in cancer therapy: The involvement of oxidative stress. J Control Release. 2022;348:287-304. https://doi.org/10.1016/j.jconrel.2022.05.035.
15. Martorana A, Perricone U, Lauria A. The repurposing of old drugs or unsuccessful lead compounds by in silico approaches: New advances and perspectives. Curr Top Med Chem. 2016;16(19):2088-106. https://doi.org/10.2174/1568026616666160216153457.
16. Bhar S. Role of Drug Repurposing in Sustainable Drug Discovery. InDrug Repurposing-Advances, Scopes and Opportunities in Drug Discovery 2023 Mar 23. IntechOpen.
17. Pushpakom S, Iorio F, Eyers PA, Escott KJ, Hopper S, Wells A, et al. Drug repurposing: Progress, challenges and recommendations. Nat Rev Drug Discov. 2019;18(1):41-58. https://doi.org/10.1038/nrd.2018.168.
18. Antoszczak M, Markowska A, Markowska J, Huczynski A. Old wine in new bottles: Drug repurposing in oncology. Eur J Pharmacol. 2020;866:172784. https://doi.org/10.1016/j.ejphar.2019.172784.
19. Ahmed ZSO, Golovoy M, Abdullah Y, Ahmed RSI, Dou QP. Repurposing of metformin for cancer therapy: Updated patent and literature review. Recent Pat Anticancer Drug Discov. 2021;16(2):161-86. https://doi.org/10.2174/1574892816666210615163417.
20. Daugan M, Dufay Wojcicki A, d'Hayer B, Boudy V. Metformin: An anti-diabetic drug to fight cancer. Pharmacol Res. 2016;113(Pt A):675-85. https://doi.org/10.1016/j.phrs.2016.10.006.
21. Song CW, Lee H, Dings RP, Williams B, Powers J, Santos TD, et al. Metformin kills and radiosensitizes cancer cells and preferentially kills cancer stem cells. Sci Rep. 2012;2:362. https://doi.org/10.1038/srep00362.
22. Zhao B, Luo J, Yu T, Zhou L, Lv H, Shang P. Anticancer mechanisms of metformin: A review of the current evidence. Life Sci. 2020;254:117717. https://doi.org/10.1016/j.lfs.2020.117717.
23. Loubiere C, Goiran T, Laurent K, Djabari Z, Tanti JF, Bost F. Metformin-induced energy deficiency leads to the inhibition of lipogenesis in prostate cancer cells. Oncotarget. 2015;6(17):15652-61. https://doi.org/10.18632/oncotarget.3404.
24. Adams JM, Cory S. The bcl-2 arbiters of apoptosis and their growing role as cancer targets. Cell Death Differ. 2018;25(1):27-36. https://doi.org/10.1038/cdd.2017.161.
25. Loubiere C, Clavel S, Gilleron J, Harisseh R, Fauconnier J, Ben-Sahra I, et al. The energy disruptor metformin targets mitochondrial integrity via modification of calcium flux in cancer cells. Sci Rep. 2017;7(1):5040. https://doi.org/10.1038/s41598-017-05052-2.
26. Nair V, Sreevalsan S, Basha R, Abdelrahim M, Abudayyeh A, Rodrigues Hoffman A, et al. Mechanism of metformin-dependent inhibition of mammalian target of rapamycin (mtor) and ras activity in pancreatic cancer: Role of specificity protein (sp) transcription factors. J Biol Chem. 2014;289(40):27692-701. https://doi.org/10.1074/jbc.M114.592576.
27. Chiang CF, Chao TT, Su YF, Hsu CC, Chien CY, Chiu KC, et al. Metformin-treated cancer cells modulate macrophage polarization through ampk-nf-kappab signaling. Oncotarget. 2017;8(13):20706-18. https://doi.org/10.18632/oncotarget.14982.
28. Pulito C, Mori F, Sacconi A, Goeman F, Ferraiuolo M, Pasanisi P, et al. Metformin-induced ablation of microrna 21-5p releases sestrin-1 and cab39l antitumoral activities. Cell Discov. 2017;3:17022. https://doi.org/10.1038/celldisc.2017.22.
29. Narmani A, Rezvani M, Farhood B, Darkhor P, Mohammadnejad J, Amini B, et al. Folic acid functionalized nanoparticles as pharmaceutical carriers in drug delivery systems. Drug Dev Res. 2019;80(4):404-24. https://doi.org/10.1002/ddr.21545.
30. Zhong S, Zhang H, Liu Y, Wang G, Shi C, Li Z, et al. Folic acid functionalized reduction-responsive magnetic chitosan nanocapsules for targeted delivery and triggered release of drugs. Carbohydr Polym. 2017;168:282-9. https://doi.org/10.1016/j.carbpol.2017.03.083.
31. Watanabe K, Kaneko M, Maitani Y. Functional coating of liposomes using a folate- polymer conjugate to target folate receptors. Int J Nanomedicine. 2012;7:3679-88. https://doi.org/10.2147/IJN.S32853.
32. Yoo HS, Park TG. Folate-receptor-targeted delivery of doxorubicin nano-aggregates stabilized by doxorubicin-peg-folate conjugate. J Control Release. 2004;100(2):247-56. https://doi.org/10.1016/j.jconrel.2004.08.017.
33. Borah PK, Das AS, Mukhopadhyay R, Sarkar A, Duary RK. Macromolecular design of folic acid functionalized amylopectin-albumin core-shell nanogels for improved physiological stability and colon cancer cell targeted delivery of curcumin. J Colloid Interface Sci. 2020;580:561-72. https://doi.org/10.1016/j.jcis.2020.07.056.
34. Koirala N, Das D, Fayazzadeh E, Sen S, McClain A, Puskas JE, et al. Folic acid conjugated polymeric drug delivery vehicle for targeted cancer detection in hepatocellular carcinoma. J Biomed Mater Res A. 2019;107(11):2522-35.

https://doi.org/10.1002/jbm.a.36758.
35. Alibolandi M, Abnous K, Sadeghi F, Hosseinkhani H, Ramezani M, Hadizadeh F. Folate receptor-targeted multimodal polymersomes for delivery of quantum dots and doxorubicin to breast adenocarcinoma: In vitro and in vivo evaluation. Int J Pharm. 2016;500(1-2):162-78. https://doi.org/10.1016/j.ijpharm.2016.01.040.
36. Selim YA, Azb MA, Ragab I, M HMAE-A. Green synthesis of zinc oxide nanoparticles using aqueous extract of deverra tortuosa and their cytotoxic activities. Sci Rep. 2020;10(1):3445. https://doi.org/10.1038/s41598-020-60541-1.
37. Islam A, Sharma A, Chaturvedi R, Kumar Singh P. Synthesis and structural analysis of zinc oxide nano particle by chemical method. Mater Today: Proc . 2021;45:3670-3. https://doi.org/10.1016/j.matpr.2021.01.281.
38. Talam S, Karumuri SR, Gunnam NJISRN. Synthesis, characterization, and spectroscopic properties of zno nanoparticles. 2012;2012:1-6.
39. Kim KM, Kim TH, Kim HM, Kim HJ, Gwak GH, Paek SM, Oh JM. Colloidal behaviors of ZnO nanoparticles in various aqueous media. Toxicology and Environmental Health Sciences. 2012 Jun;4:121-31.
40. Achehboune M, Khenfouch M, Boukhoubza I, Derkaoui I, Mothudi BM, Zorkani I, et al. Effect of yb concentration on the structural, magnetic and optoelectronic properties of yb doped zno: First principles calculation. Optical Quantum Electronics. 2021;53(12):709. https://doi.org/10.1007/s11082-021-03369-x
41. Xiong G, Pal U, Serrano JG, Ucer KB, Williams RT. Photoluminesence and ftir study of zno nanoparticles: The impurity and defect perspective. Physica Status Solidi C. 2006;3(10):3577-81. https://doi.org/10.1002/pssc.200672164.
42. Nayak AK, Pal D. Formulation optimization and evaluation of jackfruit seed starch-alginate mucoadhesive beads of metformin hcl. Int J Biol Macromol. 2013;59:264-72. https://doi.org/10.1016/j.ijbiomac.2013.04.062.
43. He YY, Wang XC, Jin PK, Zhao B, Fan X. Complexation of anthracene with folic acid studied by ftir and uv spectroscopies. Spectrochim Acta A Mol Biomol Spectrosc. 2009;72(4):876-9. https://doi.org/10.1016/j.saa.2008.12.021.
44. Palanikumar L, Ramasamy S, Hariharan G, Balachandran C. Influence of particle size of nano zinc oxide on the controlled delivery of amoxicillin. Applied Nanoscience. 2013;3(5):441-51. https://doi.org/10.1007/s13204-012-0141-5.
45. Cicero AF, Tartagni E, Ertek S. Metformin and its clinical use: New insights for an old drug in clinical practice. Arch Med Sci. 2012;8(5):907-17. https://doi.org/10.5114/aoms.2012.31622.
46. Buczynska A, Sidorkiewicz I, Kretowski AJ, Zbucka-Kretowska M, Adamska A. Metformin intervention-a panacea for cancer treatment? Cancers (Basel). 2022;14(5). https://doi.org/10.3390/cancers14051336.
47. Zhou J, Xu NS, Wang ZL. Dissolving behavior and stability of zno wires in biofluids: A study on biodegradability and biocompatibility of zno nanostructures. Advanced Materials. 2006;18(18):2432-5. https://doi.org/https://doi.org/10.1002/adma.200600200.
48. Mallik R, Chowdhury TA. Metformin in cancer. Diabetes Res Clin Pract. 2018;143:409-19. https://doi.org/10.1016/j.diabres.2018.05.023.
49. Hanley C, Layne J, Punnoose A, Reddy KM, Coombs I, Coombs A, et al. Preferential killing of cancer cells and activated human t cells using zno nanoparticles. Nanotechnology. 2008;19(29):295103. https://doi.org/10.1088/0957-4484/19/29/295103.
50. Zwicke GL, Mansoori GA, Jeffery CJ. Utilizing the folate receptor for active targeting of cancer nanotherapeutics. Nano Rev. 2012;3. https://doi.org/10.3402/nano.v3i0.18496.